

An experimental performance analysis of a cold region stationary photovoltaic system

Wongyu Choi^{*1}, Ryan D. Warren² and Michael B. Pate¹

¹Department of Mechanical Engineering, Texas A&M University, College Station, Texas, USA

²Senior Project Manager, Nexant, Chicago, Illinois, USA

(Received June 9, 2015, Revised December 4, 2015, Accepted January 21, 2016)

Abstract. A grid-connected photovoltaic (PV) system comprised of multicrystalline silicon (mc-Si) modules was installed in a cold climate region in the U.S. This roof-mounted stationary PV system is a real-world application of PV for building energy generation in International Energy Conservation Code (IECC) Climate Zone 5 (and possibly similar climate zones such as 6, 7 and 8), and it served the purposes of research, demonstration, and education. The importance of this work is highlighted by the fact that there has been less emphasis on solar PV system in this region of the U.S. because of climate and latitude challenges. The system is equipped with an extensive data acquisition system capable of collecting performance and meteorological data while visually displaying real-time and historical data through an interactive online interface. Experimental data was collected and analyzed for the system over a one-year period with the focus of the study being on measurements of power production, energy generation, and efficiency. The annual average daily solar insolation incident upon the array was found to be 4.37 kWh/m². During the first year of operation, the PV system provided 5,801 kWh (1,264 kWh/kWp) of usable AC electrical energy, and it was found to operate at an annual average conversion efficiency and PR of 10.6 percent and 0.79, respectively. The annual average DC to AC conversion efficiency of the inverter was found to be 94 percent.

Keywords: energy and power production; renewable energy; alternative energy; solar energy; energy efficiency

1. Introduction

The use of photovoltaic (henceforth, PV) technology has entered a new stage of importance and development throughout not only the U.S. but the world, regardless of climate zone, because of the introduction of net zero energy buildings (ZEB). Specifically, PV technology is currently considered an indispensable element in ZEBs (Marszal *et al.* 2011, Li *et al.* 2013) because the advantages of PV technology are integral to the concept of ZEB power generation, which is a stand-alone energy power source as well as a grid-connected power source.

Despite the widespread interest in the ZEB concept throughout the U.S., the use and research of building-integrated PV is not widespread in the colder parts of the U.S. (i.e., Upper Midwest). Part of the reason for this lack of use and research arises from the historical belief that the use of PV is

*Corresponding author, E-mail: wongyuchoi@tamu.edu

more valid in hot, dry climates because of the higher solar insolutions found in these climates. Focusing PV interest to hot, dry climates based on economic issues may have been understandable in the past, but now there is a substantial interest in ZEBs in all locations, including varied climate regions. In order to address the PV applications in the colder parts of the U.S., including the Upper Midwest, it is first necessary to categorize climate regions according to the quantitative measures such as cooling degree days and heating degree days along with temperature and humidity. The International Energy Conservation Code (IECC) has provided IECC Climate Zone criteria for such purposes (ICC 2012), where the climate zone is divided into Zone 1 through Zone 8 based on different heating degree days, cooling degree days, and moisture divisions. For example, IECC Climate Zone 5 is defined as regions having heating degree days of the base temperature 18°C (65°F in IP Units) between 3,000 and 4,000°C (5,400 and 7,200°F in IP Units), where the heating degree day is defined by the one-year summation of the daily degree difference-between the daily-mean outdoor temperature and the base temperature, only when the daily-mean outdoor temperature is less than the base temperature (ICC 2012). Of special importance, the colder part of the U.S. discussed in this study is categorized as IECC Climate Zone 5 through 8.

The need for PV research to support and promote PV usage in cold climates can be vividly demonstrated by showing the installed PV capacities for various cold-climate states in the U.S., which includes the Upper Midwest, and comparing this capacity to other locations. Table 1 is a list of U.S. states whose majority of area can be categorized in IECC Climate Zones 5 through 8 (henceforth, ICZ 5-8) along with their grid connected PV installations (Sherwood 2014) in 2013 in units of MW_{DC} (direct current megawatts). It should be noted that 37 of 50 U.S. states consist of more than one IECC climate zone. Therefore, only states whose majority of land area falls into any of ICZ 5 through 8 are included as ICZ 5-8 modified states in Table 1. For example, California (CA) includes ICZ 2 through 6; however, most counties are categorized into ICZ 3, and thus CA is not considered in the ICZ 5 through 8 group. A noticeable observation is the total grid connected installation of PV in 2013 of these modified ICZ 5-8 states is only 12.1 percent of the entire U.S. states while the cumulative installed capacity is only 17.0 percent. This clearly shows the challenges that PV installations in the colder regions of the U.S. states have experienced, especially considering that those states listed in Table 1 occupy about 70 percent (5,576,270 km²) of the U.S. land area.

In spite of the low PV usage in cold climates, several studies have pointed out that the colder climates have more potential for PV operations. Kawajiri *et al.* (2011) performed a vast geographical and meteorological study in order to explore PV application potential in various climates and geographical zones. In their study, the researchers found that cold climates have much more potential for PV usage than is currently being utilized. They also found in their research that the U.S. has a uniform distribution of PV potential (kWh/kW), which is characterized as the ratio of an annual PV energy generation in kWh and a nominal power of PV array in kW. In other words, the potential of PV usage in IECC Climate Zone 5 or other colder areas does not significantly differ from the warmer parts of the U.S. An additional plus for cold climates is that Dubey *et al.* (2013) investigated temperature dependencies of PV systems to their performance for various modules and models, and they concluded that increasing temperatures result in decreases in the PV's performance. Obviously, one can conclude that colder climates with their lower temperature have better performance for PV systems than those found in warmer climates. Combining these observations strongly suggests the use of PV as a viable energy generation option in IECC Climate Zone 5 or other colder zones (Norton and Christensen 2008). Furthermore, it can be concluded that a need exists for additional research studies to support this

Table 1 U.S. states (excluding territories) of IECC Climate Zones 5 through 8 modified and their grid connected PV installations and capacities (Sherwood 2014)

State	Capacity Installed in 2013 (DC megawatts, MW _{DC})				Cumulative Installed Capacity (DC megawatts, MW _{DC})
	Residential	Non-residential	Utility	Total	
Alaska	0.1	0.1	*	0.2	0.2
Connecticut	10.5	21.3	5.8	37.5	77.1
Idaho	0.4	0.4	*	0.7	1.8
Illinois	0.1	0.4	*	0.5	43.4
Indiana	0.8	0.4	43.8	45.0	49.4
Iowa	1.3	2.1	*	3.4	4.6
Maine	2.2	0.4	*	2.5	5.3
Massachusetts	28.7	166.7	27.3	222.6	445.0
Michigan	1.2	1.1	*	2.3	22.2
Minnesota	0.6	1.2	2.0	3.8	15.1
Montana	0.6	0.3	*	0.9	3.0
Nebraska	0.1	0.1	*	0.2	0.6
Nevada	4.8	7.5	34.6	46.9	424.0
New Hampshire	2.8	1.4	*	4.1	9.6
New Mexico	10.3	13.6	25.2	49.1	256.6
New York	24.2	33.1	3.8	61.1	240.5
North Dakota	0.1	*	*	0.1	0.2
Ohio	3.0	10.5	5.0	18.5	98.4
Oregon	4.8	1.7	*	6.4	62.8
Pennsylvania	7.3	8.5	*	15.9	180.2
Rhode Island	*	*	5.7	5.7	7.6
South Dakota	*	*	*	*	*
Utah	2.8	3.2	*	6.0	16.0
Vermont	4.6	2.2	6.7	13.6	41.5
Washington	6.5	1.4	*	7.9	27.4
West Virginia	0.4	0.1	*	0.5	2.2
Wisconsin	0.6	0.7	*	1.4	22.5
Wyoming	0.2	0.2	*	0.4	1.0
Total	119.0 (13.5%)	278.6 (28.1%)	159.9 (5.8%)	557.2 (12.1%)	2058.2 (17.0%)
Other U.S. States Total	763.8 (86.5%)	712.6 (71.9%)	2580.7 (94.2%)	4057.5 (87.9%)	10061.9 (83.0%)
U.S. Total	882.8 (100.0%)	991.2 (100.0%)	2740.6 (100.0%)	4614.7 (100.0%)	12120.1 (100.0%)

*: less than 100 kWDC or data not available.

increased usages, especially when one considers the widespread interest in ZEBs.

One of the most compelling PV studies to support the increase of PV research and

demonstration in cold climates can be found in a survey conducted in the United Kingdom (U.K.). Specifically, this survey study found that 88% of respondents would consider purchasing and using integrated photovoltaic building products (BIPV) given evidence of their performance and reliability (Fanny and Dougherty 2001). This U.K. study also showed that 49% of those surveyed would consider the use of BIPV technology only after they had witnessed the actual use of it in demonstration sites (Fanny and Dougherty 2001). Of special importance, these survey studies also showed that consumers and design professionals are often reluctant to adopt or promote a particular technology without first observing the application of that technology (Hall and Khan 2003). Although this survey was conducted in the U.K. for BIPV, it is expected that the acceptance of non-building integrated PV in the US would closely follow these same trends identified in the survey, which further demonstrate the importance of the research reported herein especially given the lack of real-world cold-climate PV studies.

In an attempt to overcome the barriers to the use of PV in cold climates (namely, real-life demonstration and performance studies), a grid-connected PV system was designed, instrumented, and installed in central Iowa, USA, categorized as IECC Climate Zone 5, this location actually represents a multitude of states across the upper Midwest of the U.S. The system was designed as a “turn-key” installation for a building energy generation application. The orientation of the system was selected to optimize for annual energy generation, and all of the PV and Balance-Of-System (BOS) equipment used in the installation is considered standard for residential and commercial applications. For example, flat-plate PV modules made of silicon nitride multicrystalline silicon (mc-Si) cells, which are the most common PV technology, were used in the study reported herein. The PV system is equipped also with an extensive data acquisition (DAQ) system that is capable of collecting accurate performance and meteorological data, archiving data in a central repository, and visually displaying real-time and historical data through an interactive online interface. This state-of-the-art instrumentation and data acquisition system is essential for an accurate evaluation of the actual PV system performance and operation.

Also reported herein are the results of a detailed performance analysis of the data taken over a full one-year period. The performance analysis of the system primarily focuses on measures of power production, energy generation, and efficiency. Furthermore, the analysis and data are presented on an instantaneous, daily, monthly, and annual basis. These data and analysis results reported herein can be used to set appropriate expectations for PV systems operating in IECC Climate Zone 5, thus allowing design professionals and consumers to make more informed decisions, which in turn could promote the use of PV systems in cold climates. Additionally, the experimental data collected can be used by others in the development, validation, and improvement of computer simulation tools.

2. Case study review

A number of PV system operations in the field (i.e., outside of a laboratory environment) have been reported over the years with the prevalent application of PV system case studies being for ZEBs. However, In addition, nearly all of these case studies were performed in regions other than the Upper Midwest, which comprises part of Climate Zone 5, where cold temperatures dominate. In addition, information is mostly limited to averaged power generation and consumption rather than showing the dynamics of metrological and electricity generation by PV systems. As a result, it is difficult to perform a complete performance analysis of the results or to expand the

conclusions to additional years or locations where the meteorological data may be different from the period of study.

In the literature search, three example case studies were identified as being of particular interest to the study reported herein due to the similarity of systems, climate zones, and locations.

One of these systems is a residence that consists of 22 PV modules with 210 watts per module, which totals 4.62 kW capacity. This system in Mount Pleasant, Iowa (Baer *et al.* 2012), which is categorized as ICZ 5, provided an average of 500 kWh/month, which resulted in an annual kWh-to-rated capacity at standard conditions of 1,299 kWh/kWp.

Another example of a PV installation in the Upper Midwest for a net ZEB application is the Lake Solar House in Evanston, Illinois (ICZ 5). This house relies on its electricity generation solely from a PV systems whose rated power is 6.4 kW, resulting in an electricity generation of 5352 kWh/yr (836.25 kWh/kWp). The annual energy balance report for this house (Revelle 2006) suggests that the maximum energy production is mostly in June, which can be attributed to the large solar insolation with relatively lower average temperatures than in July.

Several home building businesses in ICZ 5 have committed to PV installations for new ZEB construction. For example, in one location in Denver, CO more than 29 new homes have been equipped with at least 2.75 kW or more PV systems on their roofs depending on home size. One home for the case study with an installed 8.0 kW PV system resulted in 11,888 kWh/year energy savings with the PV systems (EERE, 2014). Although their energy ratings are accessible in terms of the Home Energy Rating System (HERS) and other key energy performance features, the annual generation data for these homes does not incorporate detailed PV performances based on laboratory-quality instrumentation along with detailed meteorological data.

These selected case studies show an evident viability of using PV systems for electricity generation in cold climates, especially when the PV systems are integrated with energy saving building configurations such as ZEBs. However, each of these studies is lacking varying degrees of details such that a need still exists for a more in-depth study and analysis using actual PV system performance and measured meteorological information.

3. PV system description

The PV system used in the performance analysis study reported herein is located in Ames, Iowa, at a latitude of an approximate 42 degrees North and a 93 degree of longitude West, which is categorized as IECC Climate Zone 5. Referring to this location as ICZ 5 is not descriptive enough in that it is located near the boundary of other climate regions such as 6, 7 and 8. Furthermore, the location has much more in common with the cold regions of the Upper Midwest that as a whole are less sunny than the weather regions of ICZ 5 (i.e., Colorado). This PV system has a total installed capacity of 4.6 kWp (rated at standard operating conditions) and total PV array area of 34 m² (366.2 ft²). This system was designed as three side-by-side, identical, and independently operating sub-systems. Each subsystem consists of nine 170 watt modules operated at their peak-power point and wired in series to a single inverter, with all three inverters being identical. As shown in Fig. 1 all modules are attached directly to a south-facing standing-seam white-metal roof at a slope of 36 degrees.

The system configuration presented in a one-line diagram can be seen in Fig. 2.

The flat-plate PV modules are made of silicon-nitride-multicrystalline silicon cells. Electrical and mechanical specifications for these modules are presented in Table 2.



Fig. 1 Photograph of stationary PV system

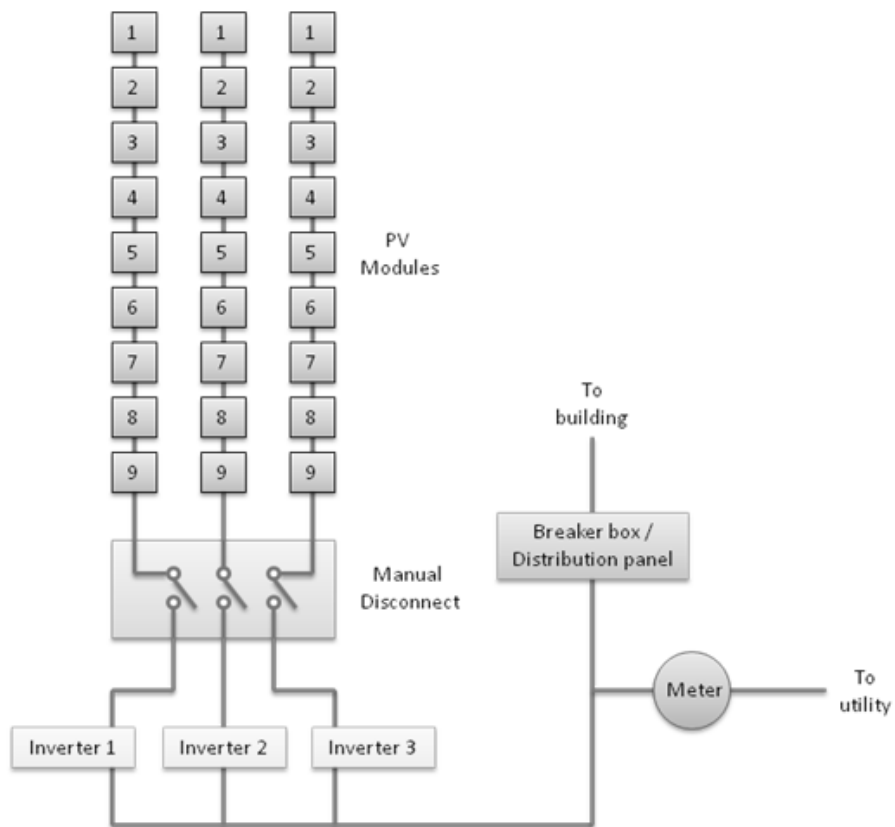


Fig. 2 One-line diagram of PV system

All three grid-tied inverters are identical and utilize maximum power-point tracking during operations. The inverters accept the DC electricity from the PV arrays and output single-phase AC electricity to the building and utility at a nominal 208 volts AC. The manufacturer's stated conversion efficiency for each inverter is 94.4 percent. Each inverter consumes less than 0.15

Table 2 Electrical and mechanical characteristics of photovoltaic modules

Rated power	170 Watts
Voltage at rated power	35.4 VDC
Current at rated power	4.8 Amps
Short-circuit current	5.0 Amps
Open-circuit voltage	44.2 VDC
Temperature coefficient of short circuit current	(0.065+0.015)%/°C
Temperature coefficient of open circuit voltage	-(160+20) mV/°C
Temperature coefficient of power	-(0.5+0.05)%/°C
NOCT (Air 20°C; sun 0.8 kW/m ² , wind 1 m/s)	47+2°C (116.6+3.6°F)
Size (length×width×depth)	1593×790×50 mm (62.8×31.1×1.97 in.)
Weight	15.0 kg (33.1 lb.)
Solar Cells	72 cells (125 mm×125 mm) in a 6×12 matrix connected in series

Table 3 Electrical and mechanical characteristics of inverters

Maximum PV input power	3,000 Watts
Operating DC voltage range	150-450 Volts DC
Maximum DC input voltage	450 Volts DC
Maximum DC input current	16.9 Amps DC
Maximum output power	2,350 Watts
Nominal output voltage	208 VAC
Utility output voltage range	196-218 Volts AC
Maximum current	11.25 Amps AC
Nominal operating frequency range	60 Hz
Power factor	1
Peak efficiency	94.4%
Power consumption in stand-by	< 0.15 Watts (night)
Power consumption during operation	7 Watts
Size (length×width×height)	470×418×223 mm. (18.5×16.46×8.78 in.)
Weight	11.79 kg. (26 lbs.)
Certifications and compliance	UL 1741, IEEE 929, ISO 9001:2000, FCC regulations

watts of electrical power in the stand-by mode and approximately 7 watts during operation. Electrical and mechanical specifications of the inverters are presented in Table 3.

The data acquisition system (DAQ) is capable of collecting accurate data, and archiving it in a central repository and visually displaying real-time and historical data through an interactive online interface. All data is measured at ten-second intervals and stored as one-minute averages. In addition, the operating parameters of the array and the meteorological conditions were monitored to adequately characterize the performance of the PV system. The specific performance parameters that were monitored include the following:

- DC voltage produced by the arrays of modules (measured at input of inverters)
- DC current produced by the arrays of modules (measured at input of inverters)
- AC voltage output by the inverters (measured at output of inverters)
- AC current output by the inverters (measured at output of inverters)
- Module temperatures

The meteorological parameters that were monitored include:

- Solar irradiance (measured at plane of array)
- Ambient air temperature
- Wind speed
- Wind direction

The placement within the system of each instrument can be seen in Fig. 3, and the operating ranges and specified accuracies of these instruments are listed in Table 4.

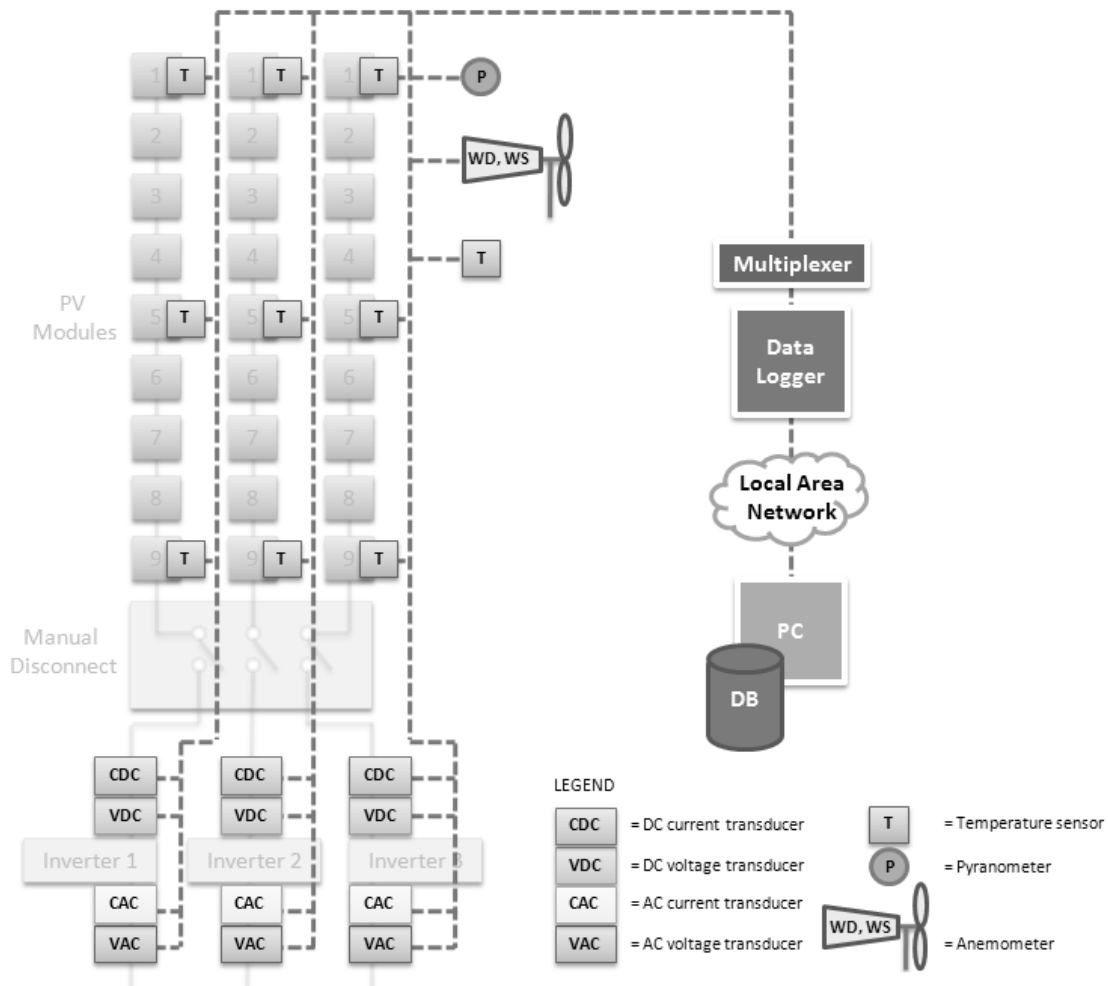


Fig. 3 One-line diagram of data acquisition system, including instrument locations

Table 4 Instrument operating ranges and accuracies

Measurement	Operating Range	Accuracy
AC current to utility	0-10 AAC	0.5% of full scale
DC current to inverter	0-5 ADC	1% of full scale
AC voltage to utility	0-300 VAC	0.5% of full scale
DC voltage to inverter	0-400 VDC	0.5% of full scale
Module temperatures	0-260°C (0-500°F)	$\pm 0.083^\circ\text{C}$ at 0°C ($\pm 0.15^\circ\text{F}$ at 32°F)
Ambient air temperature	0-260°C (0-500°F)	$\pm 0.083^\circ\text{C}$ at 0°C ($\pm 0.54^\circ\text{F}$ at 32°F)
Solar irradiance	0-1,500 W/m^2	Temp: $\pm 1\%$ from -20 - 40°C (-4 - 104°F) Linearity: $\pm 5\%$ from 0-1,500 W/m^2 Cosine: $\pm 1\%$ from 0° - 70° or $\pm 3\%$
Wind speed	1-100 m/s (2.2-224 mph)	± 0.27 m/s (± 0.6 mph) or 1% of reading
Wind direction	355° electrical	$\pm 3^\circ$

The DC wiring lengths between the modules and inverter for the first, second, and third array are 53, 65, and 74 m (174, 213, and 244 ft.), respectively. The length of DC wiring is important due to resistive losses that decrease the usable power generated by the array; however, a relatively large diameter wire was specified to minimize these effects. All of the DC wiring is insulated, uncoated 8 gauge stranded (7 conductors) copper wiring. The DC voltage and current transducers were installed at the input to the inverter. Thus, data collected by these instruments represent the actual “usable” DC electricity that could be input to an inverter, battery bank, or DC powered device and include all losses and inefficiencies between the array and inverter. The AC voltage and current were measured at the output of the inverters. However, due to the presence of reactive power in the AC current measurement, this data was not used for performance characterizations. Instead, inverter efficiency curves were generated by using data taken in a stand-alone test from a power logger capable of individually measuring working, reactive, and apparent power. The inverter efficiency model allows calculation of instantaneous inverter DC to AC conversion efficiency as a function of DC power input. Consequently, the working AC power generated by the system was calculated for each data point as a function of DC power input and inverter conversion efficiency.

4. Meteorological conditions during study period

Meteorological conditions experienced at the site during the one-year monitoring period are shown and include solar resource, ambient air temperature, wind speed and direction, and snow fall. To assess and characterize the performance of a PV system, it is important to first establish the solar resource available to the system. The solar resource to a PV system is primarily a function of geographical location, surrounding ground cover, array orientation, and atmospheric/meteorological conditions. For this research, the in-plane solar resource available to the test system was evaluated on monthly and annual bases. Monthly solar resource is presented in terms of average daily solar insolation, as shown in Fig. 4. Monthly average daily solar insolation and annual average daily solar insolation values are common parameters quantified in solar literature and are often used in PV system design. Values for these parameters have been documented for

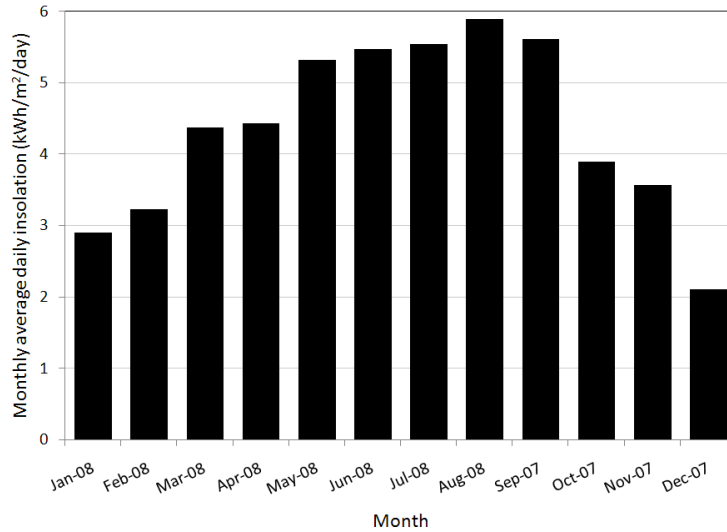


Fig. 4 Monthly average daily solar insolation

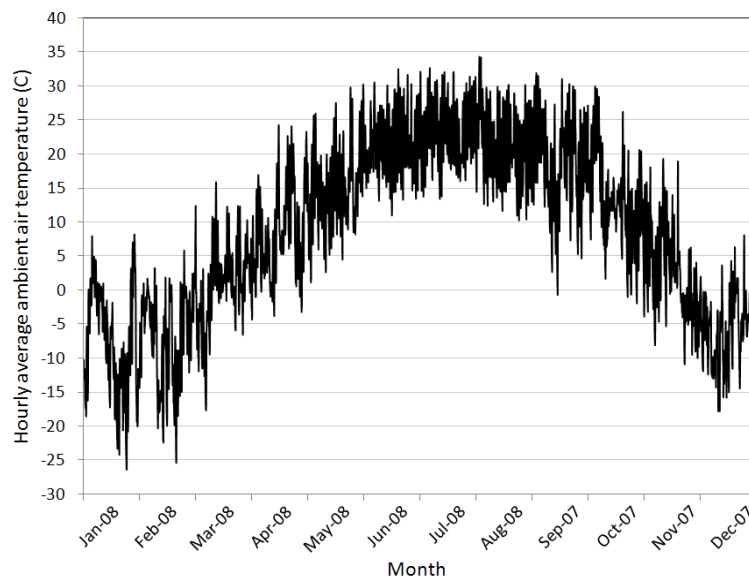


Fig. 5 Hourly average ambient air temperature

different collector types, orientations, and locations in the U.S. (Marion *et al.* 1994).

Monthly average daily solar insolutions ranged from 2.1 kWh/m² in December to 5.9 kWh/m² in August. The annual average daily solar insolation for the system was found to be 4.37 kWh/m². NREL has averaged the solar insolation over 30 years in Mason City, Iowa and Des Moines, Iowa (National Renewable Energy Laboratory 2008) and this data is used herein for comparison to the collected data. The average daily solar insolation was 4.6 kWh/m²·day for data from Mason City and 4.8 kWh/m²·day for Des Moines. The minimum for both regions is 4.2 to 4.4 kWh/m²·day. The comparison between our data and the 30 year data indicates that for the year of this

Table 5 Measured monthly average temperature during study period and national weather forecast-monthly average (National Weather Service Forecast Office 2008)

Month	Measured Ambient Air Temperature- Monthly Average °F (°C)	National Weather Forecast-Monthly Average °F (°C)
Sep-07	63.3 (17.4)	65.1 (18.4)
Oct-07	50.2 (10.1)	52.8 (11.6)
Nov-07	30.4 (-0.9)	37.9 (3.3)
Dec-07	20.1 (-6.6)	24.9 (-3.9)
Jan-08	14.5 (-9.7)	20.4 (-6.4)
Feb-08	19.8 (-6.8)	26.6 (-3)
Mar-08	32.5 (0.3)	38.4 (3.6)
Apr-08	41.9 (5.5)	50.6 (10.3)
May-08	55.0 (12.8)	61.9 (16.6)
Jun-08	66.0 (18.9)	71.4 (21.9)
Jul-08	75.2 (24.0)	76.1 (24.5)
Aug-08	74.5 (23.6)	73.1 (22.8)
Average Annual	45.3 (7.4)	49.9 (10.0)

Table 6 Measured average monthly wind speed and 66-year average (The National Climatic Data Center 1998)

Month	Average wind speed at 10 meters, m/s (mph)	1930-1996 Average wind speed in m/s (mph)
Sep-07	3.8 (8.6)	4.4 (10)
Oct-07	4.2 (9.4)	4.4 (10)
Nov-07	4.5 (10.1)	5.4 (12)
Dec-07	3.9 (8.6)	4.9 (11)
Jan-08	4.5 (10.0)	5.4 (12)
Feb-08	4.3 (9.7)	4.9 (11)
Mar-08	4.2 (9.5)	5.8 (13)
Apr-08	5.1 (11.3)	5.8 (13)
May-08	4.5 (10.1)	4.9 (11)
Jun-08	3.9 (8.8)	4.4 (10)
Jul-08	3.3 (7.3)	4.0 (9)
Aug-08	2.9 (6.4)	4.0 (9)
Annual Average	4.1 (9.2)	4.9 (10.9)

performance analysis, the average solar insolation is slightly less than the 30-year average for the region. The average peak over 30 years for the region is 5.8 in Mason City or 6.0 in Des Moines. Again, this indicates that the analysis was performed during a year where the average yearly solar insolation was less than the 30 year average. To summarize, the annual average daily solar insolation for the study year reported herein was 5 to 9% lower than the 30 year average.

The ambient air temperature and the wind speed affects module/array operating temperatures,

Table 7 Measured Monthly snow fall and meteorological snowfall recorded since 1884 (National Weather Service Forecast Office 2008)

Month	Snow fall, cm. (in.)	Average snow fall since 1884, cm. (in.)
Sep-07	0	0
Oct-07	0	1.0 (0.4)
Nov-07	12.2 (4.8)	11.4 (4.5)
Dec-07	35.8 (14.1)	19.6 (7.7)
Jan-08	28 (11)	22.4 (8.8)
Feb-08	57.7 (22.7)	20.8 (8.2)
Mar-08	12.2 (4.8)	10.4 (4.1)
Apr-08	2.8 (1.1)	6.9 (2.7)
May-08	0	0
Jun-08	0	0
Jul-08	0	0
Aug-08	0	0

which in turn influences PV system performance. The hourly average ambient air temperature experienced during the monitoring period can be seen in Fig. 5.

Table 5 shows the monthly average temperature taken from the National Weather Forecast Office. As can be seen, the average temperatures were cooler than the yearly averages up to 3.9°C (7°F). In addition, average temperatures in each month were in general cooler than the National Weather Forecast temperatures. However, in August the measured ambient temperature exceeded recorded National Weather Forecast temperature.

The average monthly wind speed and prevailing direction (at a height of 10 meters) during the year of monitoring measured in Des Moines, Iowa (which is 56 km (35 mi) from the site of the stationary system) is shown in Table 6. The table also includes the average wind speed over 66 years (The National Climatic Data Center 1998). As can be seen, the average wind speed for the year was 0.8 m/s (1.8 mph) less than that of the 66-year average.

Snow significantly affects the PV system performance in that snow cover surrounding a PV array can increase the available solar energy incident upon the array via reflection. However, of greater concern is the fact that snow covering the array can degrade the system performance considerably. Monthly snow fall measured in Des Moines, Iowa is documented in Table 7. The recorded, monthly average snow fall is also listed in Table 7, taken from the national weather service station (National Weather Service Forecast Office 2008).

5. Experimental analysis and results

Experimental data was collected for one full year with performance parameters and meteorological conditions being monitored for one year. Data was sampled at 10-second intervals and stored as one-minute averages. The PV system was new at the onset of data collection. Of special importance, the system was allowed to operate as a real-world system during the test period; modules were never cleaned of snow or soiling, and operation was not purposely

interrupted for any reason.

A detailed analysis of system performance is presented herein with the experimental performance of the PV system is quantified in terms of array current-voltage characteristics, power production, energy generation, and system and inverter efficiencies. The results are presented on hourly, daily, monthly, and annual bases where applicable.

5.1 System performance at standard test conditions

Manufacturers rate the performance of PV modules under conditions known as Standard Reporting Conditions (SRC) or Standard Test Conditions (STC) (Whitaker 1992). The specific standard test conditions used by manufacturers are: solar irradiance of $1,000 \text{ W/m}^2$, reference solar spectral irradiance air mass 1.5 (according to ASTM G-173-03), a zero-degree angle of incidence (AOI), and cell junction temperature of 25 degrees Centigrade. However, operating conditions experienced in practice rarely reflect STC, which are more applicable to laboratory testing rather than to real-world operations. Additionally, systems do not output rated DC power to the inverter at STC due to losses and inefficiencies. Furthermore, the inverter and AC-side wiring and connections introduce additional losses, causing AC power output to the building or grid to be less than DC power input to the inverter.

During the one-year monitoring, total nine incidents, which were the total 540 seconds of measurement, were found where the system was operating at full-sun 1.0 kW/m^2 ($\pm 3 \text{ W/m}^2$) and

Table 8 Performance of PV system operating at $1,000 \text{ W/m}^2$ and 25°C

Parameter description	Value at STC	Units
System DC power output (system rating 4,600 Watts DC)	4,029	Watts DC
Average DC power output per sub-system (sub-system rating 1,530 Watts DC)	1,343	Watts DC/sub-system
Average DC power output per square meter (per m^2 rating 134.92 Watts DC)	118	Watts DC/ m^2
Average DC power output per module (module rating 170 WDC)	149	Watts DC/module
Average output voltage DC per sub-system	304	Volts DC
Average output voltage DC per module	34	Volts DC
Average output current DC per sub-system	4.42	Amps DC
System AC power output	3,853	Watts AC
Average AC power output per sub-system	1,284	Watts AC/sub-system
Average AC power output per square meter	113	Watts AC/ m^2
Average AC power output per module (module rating 170 WDC)	143	Watts AC/module
Derate factor to inverter (DC side)	0.876	Fraction of rated cap.
Derate factor to utility (System)	0.838	Fraction of rated cap.
Conversion efficiency of sun energy to electrical energy to inverter (DC side)	0.119	%/100
Conversion efficiency of sun energy to electrical energy to utility (System)	0.113	%/100

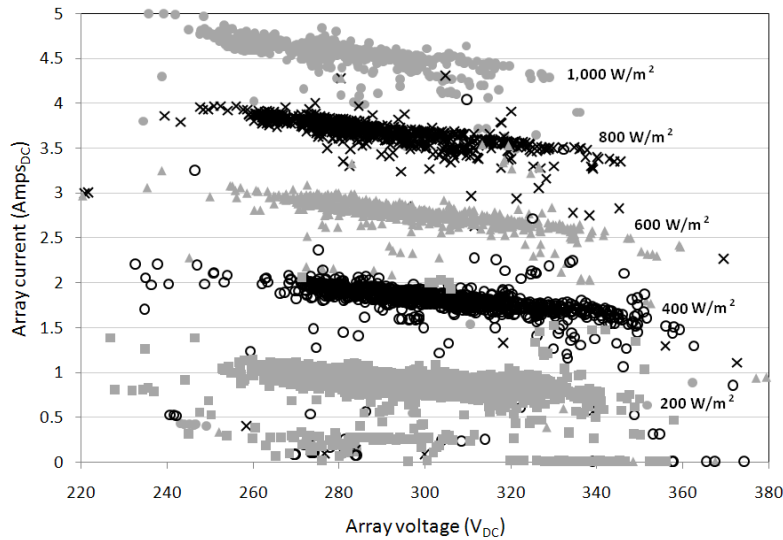


Fig. 6 I-V curves for various levels of solar irradiance

25°C ($\pm 0.25^\circ\text{C}$). The number of the nine measurement incidents of the full sun at 25°C was attributed to the relatively lower solar resource and the cold-climate characterized by ICZ 5. The measured DC and AC electrical performance data for all instances were averaged to a single value and the results are presented in Table 8.

The DC electrical parameters were measured at the input of the inverter, which means that these values represent the actual “usable” DC electricity that could be input to an inverter, battery bank, or DC powered device and include all losses and inefficiencies before the inverter. Data in this study indicates the system outputs DC power at roughly 87 percent of its rated capacity when subjected to near STC.

The average angle of incidence (AOI) calculated for the measurement intervals operating full-sun and 25°C were found to be 16 degrees. Angle of incidence values were calculated by using methods presented by Duffie and Beckman (Duffie and Beckman 1991). The AOI values do not exactly represent STC; however, past research shows this parameter to have little effect on performance at AOI’s of less than approximately 60 degrees (King and Eckert 1996, King *et al.* 2002) than other systematic losses aforementioned.

5.2 System Current-Voltage curves

A common way to characterize the electrical performance of a PV device is by measuring the current-voltage curve (I-V) at standard conditions (Del Cuerto and McMahon 2002). However, this is most often done in an indoor laboratory setting where the operating environment is controlled to specific conditions and where the performance is unaffected by external hardware, such as a battery bank or inverter. In this research, system I-V curves were generated to show actual operating performances when the array is subjected to outdoor conditions and when it is affected by inverter power point tracking. Electrical operating characteristics of the array are dictated by the maximum power point tracking (MPPT) software embedded in the inverters. The MPPT software optimizes the operating voltage of the array to achieve maximum power output at all

times.

Array operating I-V curves were generated for solar irradiance values of 200, 400, 600, 800, and 1,000W/m² (± 3 W/m²) and include data for all other operating conditions experienced throughout the year. The operating current and voltage monitored at the input of the inverter for each of the three arrays were found and averaged for each minute of data collected at the specified levels of solar irradiance as shown in Fig. 6.

Data points on Fig. 6 that do not follow the general trends correspond to times where snow partially or fully covered the array and/or the pyranometer, which was verified by comparing the sampled data points to those days when the site experienced snow fall (National Weather Service Forecast Office 2008).

5.3 Power production

The instantaneous DC and AC power production of the array was calculated from data rather than being directly measured by a single instrument. Direct current power output of the array, P_{DC}, was determined by the product of DC current and DC voltage. The AC power output of the array, P_{AC}, was found by using the DC power input to the inverter and the inverter efficiency model by

$$P_{AC} = P_{DC}\eta_{inverter} \quad (1)$$

where $\eta_{inverter}$ is the instantaneous inverter efficiency to the corresponding DC power input. The method used for calculating inverter efficiency is discussed in the later section of this paper.

The average DC power output of the system for each hour of the one-year monitoring period is plotted against corresponding hourly average in-plane solar irradiance values as shown in Fig. 7. It should be noted that the AC power output would be slightly lower for all data points because of the inverter efficiencies.

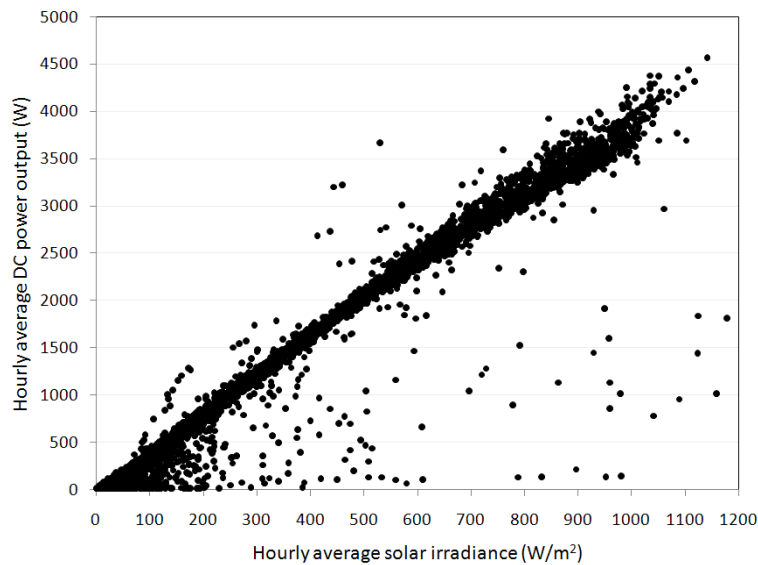


Fig. 7 Power production vs. solar irradiance

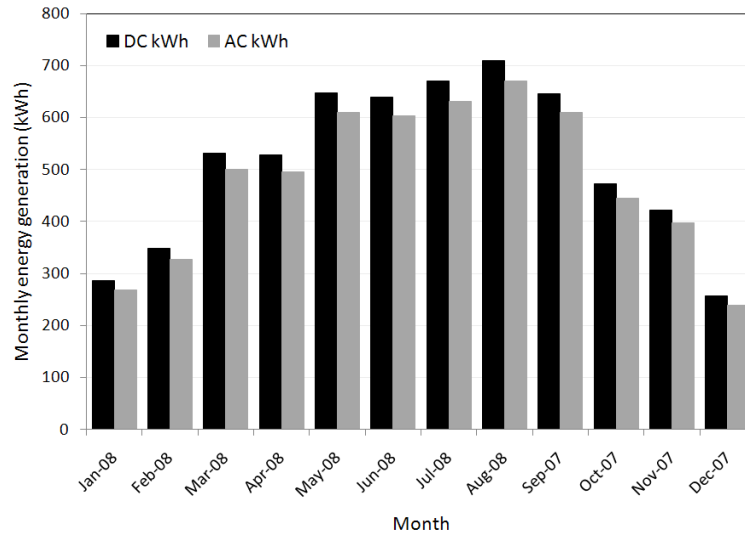


Fig. 8 Monthly energy generation

The system power productions for all operating conditions experienced at the site throughout the year are shown in Fig. 7 in terms of hourly averages of the solar irradiance (W/m^2) and DC power output (W). It can be seen in Fig. 7 that some data points deviate from the general trend with these deviations reflecting either a better or worse situation compared to the typical operation efficiencies, which can be observed as a bold linear trend in Fig. 7. Points under the linear trend in Fig. 7 correspond to times when snow partially or fully covered the array and/or pyranometer, thus affecting a lesser power production or measured irradiance as a consequence of this soiling. Points located over the linear trend, which reflects more power production, are of a much less number than the opposite deviations of being under the line. The number differences can be described by the physics of the PV polarized curve (I-V curve), where it is more likely to have losses to the rated power generation because of energy losses shunt, mismatch, series, etc.

The maximum hourly average AC and DC power output of the system was measured to be 4.36 and 4.58 kW (corresponding to a solar irradiance of $1.14 \text{ kW}/\text{m}^2$ and an average array temperature of 18°C (64°F)), respectively. The average AC and DC power output of the system at full sun (i.e., $1.0 \text{ kW}/\text{m}^2$) was found to be 3.65 and 3.81 kW, respectively.

5.4 Energy generation

The array performance was also characterized in terms of energy generation, which was evaluated for different time intervals (i.e., monthly and annually) and against solar energy input to the system. Monthly and annual AC and DC energy generation was calculated by multiplying the instantaneous power production value by the time-interval for which the power was produced, and then summing these values over the month or year. Results for monthly energy generation are shown in Fig. 8.

Two different seasonal groups can be observed in Fig. 8 in terms of the amount of the energy generation, namely the sunny season from March to September and the cold season, with reduced daylight hours, from October to February. However, as shown in the earlier meteorological

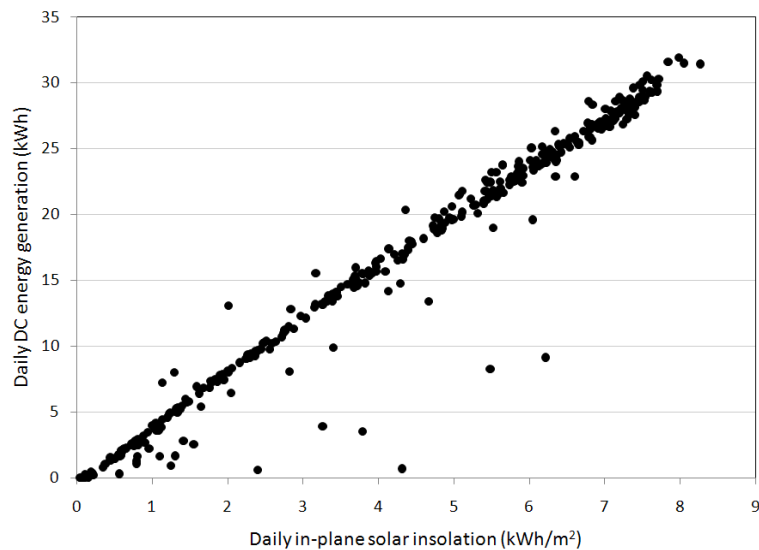


Fig. 9 Daily DC energy generation vs. daily in-plane solar insolation

discussions with Fig. 5 and Table 5, energy productions in October and November can vary depending on annual climate condition. It is possible to have more energy production in the near future because the test year was a less-sunny year as shown in Fig. 4. As an aside, the annual AC and DC energy generation for the system was found to be 5,801 and 6,162 kWh (1,264 and 1,342 kWh/kWp), respectively.

The daily DC energy generation of the system was evaluated against the daily in-plane solar insolation incident on the array as shown in Fig. 9.

As discussed before the effects of snow cover are evident by the fact that some data points fall below the main trend line. Also shown in Fig. 9 is that the relationship between daily DC energy generation and daily solar insolation is approximately linear. The deviations from the main trend line were observed in Fig. 7 because of the instantaneous time-integration of PV electrical power and energy generation. Therefore, same reasons as previously noted for Fig. 7, soiling such as snow-cover with energy losses from shunt, mismatch, series, etc., can explain this phenomenon.

5.4.1 Performance model

A performance model was developed to predict the performance of stationary PV systems. Performance parameters that were modeled include monthly and annual average daily solar insolation along with monthly and annual AC energy generation (kWh).

The total solar radiation striking the photovoltaic array can be split into two components, namely beam and diffuse radiation. The beam radiation is the portion of the total solar radiation striking the array without having been scattered by the atmosphere and is known as direct solar radiation (Duffie and Beckman 1991). The diffuse radiation is the portion of the total solar radiation striking the array after its direction has been changed due to scattering by the atmosphere, and it is known as solar sky radiation (Duffie and Beckman 1991). Thus, the total irradiance, which is the rate at which radiant energy is incident on a surface per unit area of surface, is the sum of the beam and diffuse radiation rates incident on the array per unit area.

All solar data for the model was obtained from the National Renewable Energy Laboratory

(NREL) Typical Meteorological Year 3rd Edition (TMY3) data set. The TMY3 data has been used by others in a variety of energy performance software (Wilcox and Marion 2008, Lubitz 2011, Jakubiec and Reinhart 2013). Also, the datasets are in a text file format, and there is an individual file for 239 cities in the United States.

The TMY3 data gives solar values for a horizontal surface; therefore, the amount of solar radiation incident on a tilted surface, (e.g., a fixed photovoltaic array), must be modeled. Methods for estimating solar insolation on a tilted surface are based on work done by Duffie and Beckman (Duffie and Beckman 1991). For example, the hourly beam radiation incident on a tilted surface can be determined by

$$I_{b,T} = I_b R_b \quad (2)$$

The parameter R_b represents the ratio of beam radiation on a tilted surface to that on a horizontal surface for a particular hour and was determined by

$$R_b = \frac{I_{b,T}}{I_b} = \frac{\cos \theta_i}{\cos(\theta_z)_i} \quad (3)$$

The angle of incidence, θ , is the angle between the beam radiation on a surface and the normal to that surface; whereas, the zenith angle, θ_z , is the angle between the vertical and the line to the sun. The angle of incidence and the zenith angle were determined by

$$\cos \theta_i = \begin{pmatrix} \sin \delta_i \sin \phi \cos \beta - \sin \delta_i \cos \phi \sin \beta \cos \gamma \\ + \cos \delta_i \cos \phi \cos \beta \cos \omega_i + \cos \delta_i \sin \phi \sin \beta \cos \phi \cos \omega_i \\ + \cos \delta_i \sin \phi \sin \beta \sin \omega_i \end{pmatrix} \quad (4)$$

$$\cos(\theta_z)_i = \cos \phi \cos \delta_i \cos \omega_i + \sin \phi \sin \delta \quad (5)$$

The Greek term omega, ω , is the angular displacement of the sun east or west of the local meridian, and it is due to the rotation of the earth on its axis at 15 degrees per hour. The angular displacement value is calculated in radians where the morning values are negative and the afternoon values are positive by

$$\omega_i = (\text{Solar Hour} - 12) \times 15^\circ \quad (6)$$

The solar time, which is used in all of the sun-angle relationships, is the time based upon the rotation of the earth around the sun. When the sun is the highest in the sky, it is solar noon. The difference between standard time and solar time can be determined by

$$\text{Solar Time} - \text{Standard Time} = 4(L_{st} - L_{loc}) + E \quad (7)$$

where the equation of time, E , is

$$E = 229.2 \begin{pmatrix} 0.000075 + 0.001868 \cos B - 0.032077 \sin B \\ -0.014615 \cos 2B - 0.04089 \sin 2B \end{pmatrix} \quad (8)$$

and B is

$$B = (n - 1) \frac{360}{365} \quad (9)$$

The standard meridians, L_{ST} , for the continental U.S. time zones are: Eastern, 75°W; Central, 90°W; Mountain, 105°W; and Pacific, 120°W. The declination, δ , is the angular position of the sun with respect to the plane of the equator with north being positive at solar noon.

$$\delta_i = 23.45 \sin \left(360 \frac{284 + n}{365} \right) \quad (10)$$

The latitude, ϕ , gives the location on the earth north or south of the equator, which is expressed in degrees and minutes. The slope of the array surface is denoted by using β . The surface azimuth angle, γ , is the deviation of the projection on a horizontal plane of the normal to the surface from the local meridian, with zero due south, east negative, and west positive (Duffie and Beckman 1991). This value can also be determined using a GPS device.

Any beam insolation values that were calculated and corresponded to a negative $\cos\theta$ or $\cos\theta_z$ were set to zero. This was done because negative values for these parameters indicate that either the sun has gone under the horizon or the sun is behind the surface so that there is no incident beam radiation on the surface.

The hourly diffuse radiation on a tilted surface was determined by

$$I_{d,T} = I_d \left(\frac{1 + \cos\beta}{2} \right) + I_{\rho g,i} \left(\frac{1 - \cos\beta}{2} \right) \quad (11)$$

The ground reflectance, ρg , was estimated assuming two conditions, grass and snow covered. The hourly snow depth values from the TMY3 data were used to determine if the ground was snow covered. If the snow depth for the hour was found to be greater than zero, then the ground reflectance was assumed to be 0.7; otherwise, the ground was assumed to be grass covered with an approximate ground reflectance value of 0.25. All of the hourly diffuse values that corresponded to a negative $\cos\theta_z$ value were set to zero.

The total solar energy striking the array was found by the summation of the beam and diffuse components

$$I = I_{b,T} + I_{d,T} \quad (12)$$

The model estimates the monthly and annual energy production of the assumed photovoltaic system. Using the solar model, the solar insolation for each month and annually can be determined. A full-sun hour is an hour when the sun is emitting approximately 1000 W/m² (i.e., 3.6 MJ/m² in an hour). The daily average full-sun hours for each month are calculated by

$$\left(\frac{\text{Average Full Sun Hours}}{\text{Day}} \right)_m = \frac{1}{3.6u} \sum_{i=1}^{\text{Hrs.in mo.}} (I_{T,i}) \quad (13)$$

where I_T is in units of MJ/(hr·m²).

The daily average full-sun hours over the entire year are calculated by

$$\left(\frac{\text{Average Full Sun Hours}}{\text{Day}} \right)_m = \frac{1}{1314} \sum_{i=1}^{8760} (I_{T,i}) \quad (14)$$

The efficiency of each of the components in the system is considered by using de-rate factors. An overall de-rate factor is found by the product of the individual de-rate factors with the overall de-rate factor being calculated by (Marion *et al.* 2005)

Table 9 Model inputs

Input variables	Input value
DC sub-array orientation	Stationary
State	Iowa
City	Des Moines
System type	Stationary
Array installed size (kWp)	4.59
Slope (deg.)	36
Azimuth (deg.)	0 (due south)
Module manufacturer	BP Solar
Module model number	SX170B
Inverter manuf.	Fronius USA, LLC
Inverter model number	IG 2500-LV
Overall derate factor	0.78
Normalized project cost (\$/Wp)	8.98
Annual O&M (% of initial cost)	0.1
Initial rebate amount (\$)	0
System life (years)	25
Electric rate (\$/kWh)	0.12
Inflation rate (%)	4
Sector	Commercial
Loan	No

$$\begin{aligned}
\text{Derate Factor} = & \eta_{DC\text{ rating}} \cdot \eta_{inverter} \cdot \eta_{mismatch} \cdot \eta_{diodes} \cdot \eta_{DC\text{ wiring}} \\
& \cdot \eta_{AC\text{ rating}} \cdot \eta_{soiling} \cdot \eta_{soiling} \cdot \eta_{system\text{ availability}} \cdot \eta_{shading} \\
& \cdot \eta_{age} \cdot \eta_{suntracking}
\end{aligned} \tag{15}$$

Finally, the estimated energy output from the array is

$$\frac{\text{Energy Produced}}{\text{year}} = \left(\frac{\text{Avg. full sun hours}}{\text{day}} \right) \left(\frac{365}{\text{year}} \right) (P_{rated}) (\text{Derate Factor}) \tag{16}$$

where P_{rated} is rated power in kW_p. It should be noted that the unit in Eq. (16) of each hand side is kWh/yr.

5.4.2 Comparison of model and experimental results

The experimental performance of the system was compared to predictions made by the model. A summary of the inputs used for the system simulation is shown in Table 9.

The system was assumed to operate in Des Moines, Iowa, which is the closest location to the actual site where TMY3 data is available. Actual PV system sizes, orientations, and equipment that were presented earlier were used. Additionally, the default overall derate factor calculated in the model was used; actual annual average derate factors (i.e., performance ratios) were known but

Table 10 Modeled vs. experimental solar insolation and energy generation

Month	Solar insolation			AC energy generation		
	Modeled	Experimental	% diff.	Modeled	Experimental	% diff.
Jan	98	90	9.2	351	260	35.2
Feb	116	90	29.0	417	326	27.9
Mar	140	136	3.6	501	501	0.1
Apr	154	133	16.1	551	496	11.0
May	173	165	5.0	618	611	1.2
Jun	179	164	9.2	640	603	6.1
Jul	193	172	11.9	688	632	8.9
Aug	173	183	-5.2	619	671	-7.7
Sep	151	168	-10.6	538	611	-11.9
Oct	132	121	9.1	470	446	5.4
Nov	93	107	-13.3	331	397	-16.7
Dec	86	65	31.3	306	239	28.1
Annual	1,690	1,594	6.0	6,031	5,792	4.1

would not normally be known by a user without experimental data.

The experimental performance results and modeled predictions for the PV system are presented in Table 10.

It can be seen in Table 10 that on an annual basis model predictions for solar insolation and energy generation differed from experimental results by 6 and 4.1 percent, respectively. However, on a monthly basis the differences between modeled and experimental results were larger, varying from 3.6 to 31.3 percent and 0.1 to 35.2 percent for the solar insolation and AC energy generation, respectively. Even so, many of the monthly percent differences are less than 10 percent.

Discrepancies in performance between experimental and modelled energy generation can be attributed in part to snow cover affecting experimental performance and to differences in solar insolation. During the winter months, the system was exposed to snow fall, and greater differences in energy generation can be seen in Table 10 during that time. The average differences in energy generation for the PV system for those months when no snow fall occurred (May through October) were found to be less than 7 percent. However, during those months when snow fall occurred at the site (January, February, March, April, November, and December) the average discrepancy in energy generation for the system was found to be about 20 percent. Additionally as expected, those discrepancy trends can be seen between solar insolation and energy generation. For those months when experimentally measured solar insolation differed greatly from predicted solar insolation, then for these same months energy generation discrepancies were also found to be greater as can be observed in Table 10.

5.5 Efficiency analysis

System and component efficiencies are important to consider when characterizing the performance of PV systems. Efficiency assessments offer insights into energy flows and to how well the system converts the available solar resource to useable electrical energy. Losses and

Table 11 Monthly and annual average system conversion efficiencies

Month	Conversion efficiency from sun energy to DC electrical energy (percent)	Conversion efficiency from sun energy to AC electrical energy (percent)
Sep-07	11.3	10.7
Oct-07	11.5	10.9
Nov-07	11.6	10.9
Dec-07	11.5	10.7
Jan-08	9.0	8.5
Feb-08	11.3	10.6
Mar-08	11.5	10.9
Apr-08	11.7	11.0
May-08	11.5	10.9
Jun-08	11.5	10.8
Jul-08	11.4	10.8
Aug-08	11.4	10.8
Annual	11.3	10.7

inefficiencies resulting in performances that are less than rated can be attributed to: inaccurate nameplate ratings, conversion from DC to AC electricity in the inverter, module mismatch, diodes, wiring and connection losses, soiling, snow cover, age, high operating temperatures, and other losses from converting solar energy to usable electrical energy (National Renewable Energy Laboratory 2008).

5.5.1 Seasonal and annual energy conversion efficiencies

As shown in Table 11, the system efficiency was quantified in terms of both average monthly efficiencies and an annual efficiency. Furthermore, DC and AC system conversion efficiencies were found. System conversion efficiency is defined as the ratio of the total DC or AC generated energy to the total solar insolation incident on the array.

The annual average DC and AC efficiencies shown in Table 11 are 11.3 and 10.7 percent, respectively. Also, slight seasonal variations can be observed in the system efficiencies in Table 11, with variation being from 0.090 to 0.117 and 0.085 to 0.110 for Sun-DC conversion and Sun-AC conversion efficiencies, respectively. For example, system efficiencies in the summer months were found to be slightly lower when compared to Spring and Fall up to 0.4 and 0.2 percent less respectively. The lower summer efficiency can be attributed in part to higher average array operating temperatures in the summer. The effects of snow cover are apparent in the lower efficiency results during January, with DC and AC efficiencies of 9% and 8.5% respectively, when the site experienced 28 cm (11 in) of snow fall.

5.5.2 PV system efficiency for different solar irradiances

System efficiency was also evaluated and quantified against solar irradiance. The system efficiency curve was generated by using the ratio of average hourly AC power output to average hourly total solar insolation incident upon the array. Average hourly system efficiencies for all daylight hours of the monitoring period are shown in Fig. 10.

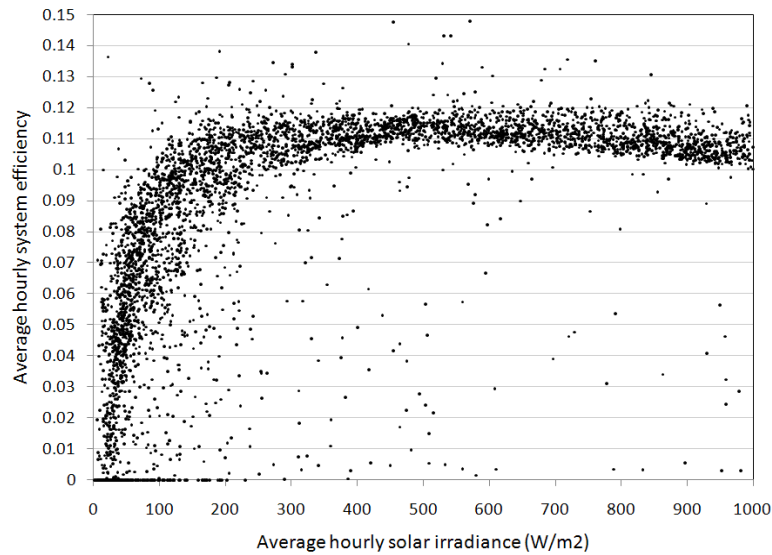


Fig. 10 System efficiency (conversion of solar energy to AC electrical energy) vs. solar irradiance

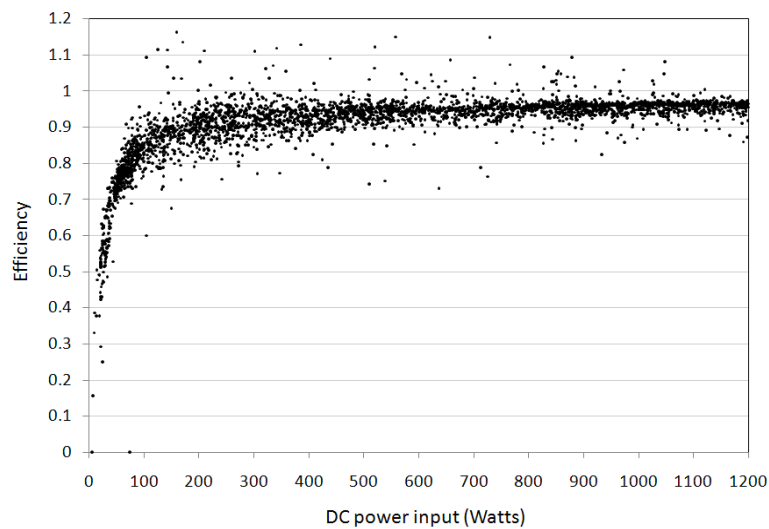


Fig. 11 Inverter efficiency vs. DC power input from array

The effects on system efficiency of influences such as array temperature, AOI, and solar spectrum can be seen by the variation of values within the main trend line. Snow cover on the array also significantly affected hourly average system efficiency, which can be seen by the data points lying below the main trend. Points that lie above the main trend line are most likely due to the intermittency of snow covering the pyranometer.

5.5.3 Inverter efficiency

Inverter performance was quantified in terms of a conversion efficiency from DC to AC electrical power. The DC and AC electrical data collected to calculate this instantaneous inverter

efficiency was measured by using an independent power logger in a stand-alone test. The conversion efficiency of each inverter was found as a function of DC power input. A plot showing results for one of the three inverters is presented in Fig. 11. This plot shows instantaneous inverter efficiency by using data at one-minute time steps. The inverters were found to operate at a fairly constant efficiency for solar irradiances ranging from 200 to 1,200 W/m², which represents a large portion of the operating range. The annual average conversion efficiency of each inverter was calculated as the ratio of annual AC energy to the annual DC energy, and it was found to be approximately 94 percent.

5.5.4 Seasonal performance ratio

The performance ratio, PR, is a parameter that is normalized with respect to irradiance and quantifies the overall effect of all losses on the rated output due to system inefficiencies, losses, and operating conditions (Marion *et al.* 2005). Performance ratio values are commonly quantified on annual, monthly, weekly, and daily bases. Longer term (i.e., annual and monthly) PR values can be used to assess the performance of a system or compare the performances of systems with similar or dissimilar characteristics and locations. Additionally, long term PR values can be estimated rather than measured to predict the energy performance of a PV system. Shorter term (i.e., weekly and daily) PR values can be used to identify component failures and other operating conditions that significantly degrade system performance such as excessive soiling or snow cover. The performance ratio can be calculated by

$$PR = \frac{Y_f}{Y_r} \quad (17)$$

where Y_f is the system yield (kWh/kWp) and Y_r is the reference yield (hours) (Marion 2005). The system yield is found by dividing the net AC energy output by the installed DC capacity of the

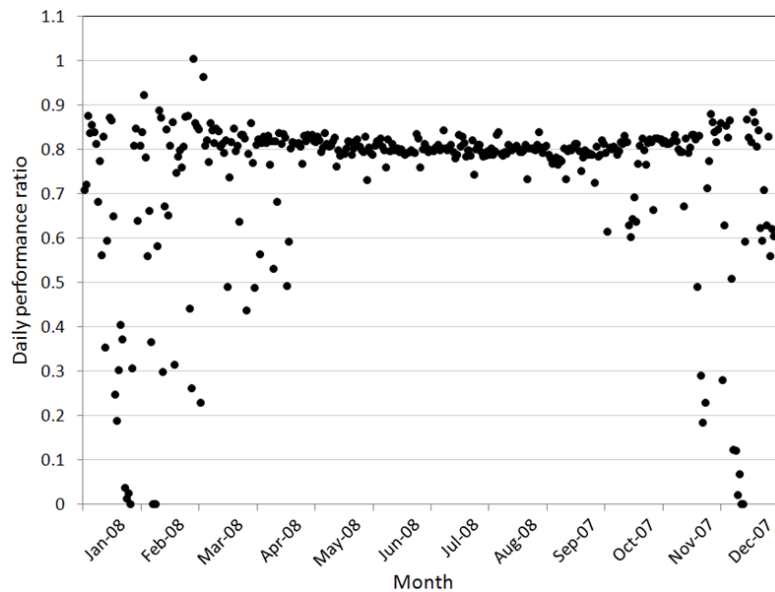


Fig. 12 Daily performance ratios

Table 12 Monthly performance ratio

Month	Average PR
Sep-07	0.790
Oct-07	0.804
Nov-07	0.810
Dec-07	0.796
Jan-08	0.629
Feb-08	0.786
Mar-08	0.805
April-08	0.814
May-08	0.806
June-08	0.800
July-08	0.800
Aug-08	0.800
Annual	0.792

array (defined at STC) (Marion *et al.* 2005). The reference yield represents the number of peak sun hours seen by the system evaluated over the same time period used for determining the system yield. Annual, monthly, and daily PR values were determined with daily PR values throughout the one-year monitoring period shown in Fig. 12. Most of daily PR values are between 0.8 and 0.9. Only a few PR values are over 0.9, and PR values lower than 0.8 occurred mostly in the winter season. PR values near 0 denotes snow fully covering the entire PV module, which resulted in zero energy generation.

It should be noted that several occasions of extremely low PR values does not render the usage of PV useless in seasons having snowfall. Rather, longer-term PR analysis is necessary to evaluate the efficiency of the PV system in each season, especially with seasons having heavy snowfall. In order to study average seasonal effects, all performance ratios calculated on monthly and annual bases are shown in Table 12.

Daily PR values during the winter months shown in Fig. 12 were found to be sporadic; the days yielding irregular PR values coincided with times the array and/or pyranometer was fully or partially covered with snow. When looking in terms of monthly PR in Table 12, however, the sporadic daily PR values had only marginal effects on the winter season, except for the extreme case of snowfall in January, 2008. Another observation is that higher PR values are observed in cooler seasons while the other months showed an almost constant PR near 0.8. These observations can be combined with earlier discussions on the meteorological conditions and the PV energy productions. Because the region where the PV measurements were taken is a cold region, namely IECC Climate Zone 5, the temperature of PV module is significantly lower than other sunnier regions in U.S. Therefore, module efficiencies could have been benefited by the low temperatures, which can explain the highest PR of 0.814 in April. To summarize, monthly PR values varied from 0.629 to 0.814 throughout the year, and the annual average performance ratio was found to be 0.792. A frequency distribution of daily PR values is shown in Fig. 13. The system was found to operate at a performance ratio level between 80 and 90 percent for 261 of the 365 day one-year monitoring period.

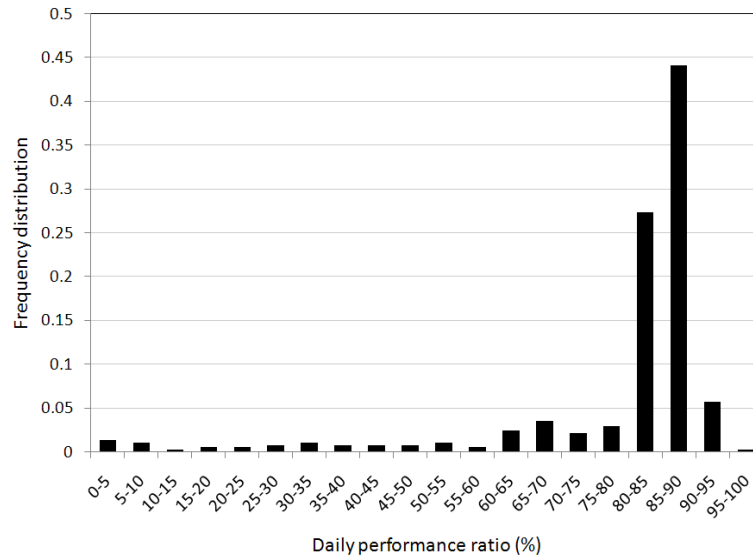


Fig. 13 Frequency distributions of performance ratios

6. Conclusions

A 4.59 kWp grid-connected, stationary PV system was installed, operated, and monitored for one year in a cold region in the upper Midwest of the U.S., defined as IECC Climate Zone 5. The array faced south and was oriented at a slope of 36 degrees in order to maximize annual energy generation. All PV and Balance-Of-System (BOS) equipment used in the installations are “off-the-shelf” components and considered standard for residential and commercial applications. What makes this installation different from other real-world setups is that it is configured with extensive instrumentation and data acquisition system. The outdoor experimental performance of the system was quantified for one year of collected data. Experimental results reflect the performance of a PV system exposed to a wide-range of operating conditions inherent to the climate in IECC Climate Zone 5 or equivalent.

The annual average daily solar insolation incident upon the array was found to be 4.37 kWh/m², and during the first year of operation, the PV system provided 5,801 kWh (1,264 kWh/kWp) of usable AC electrical energy. The system was found to operate at an annual average conversion efficiency and PR of 10.6 percent and 0.79, respectively. Slight seasonal variations in system efficiency were observed and can be attributed in part to variations in average array operating temperatures and snow fall throughout the year. The annual average DC to AC conversion efficiency of the inverter was found to be 94 percent.

The research reported herein serves several important purposes aimed at alleviating some of the current barriers to the widespread use of PV. This research can be used to set appropriate expectations for PV systems operating in colder region, defined not only by IECC Climate Zone 5 but also Zones 6 through 9, thus allowing design professionals and consumers to make more informed decisions. The test systems and results serve as demonstrations of real-world PV applications for building energy generation and are used for research, demonstration, and education purposes.

References

- Baer, N., Heide, G., Dana, R., Ryan, D., Challender, M. and Else, S.J. (2012), *Renewable Energy Incentive Rates: Potential Opportunities for Iowa Farmers*, Iowa Environmental Council, Des Moines, IA, USA.
- Del Cueto, J. and McMahon, T. (2002), "Analysis of leakage currents in photovoltaic modules under high-voltage bias in the field", *Prog. Photovoltaics*, **10**(1), 15-28.
- Dubey, S., Sarvaiya, J.N. and Seshadri, B. (2013), "Temperature dependent photovoltaic (PV) efficiency and its effect on PV production in the world-a review", *Energy Procedia*, **33**, 311-321.
- Duffie, J.A. and Beckman, W.A. (1991), *Solar Engineering of Thermal Processes*, John Wiley & Sons, Inc., New York.
- Fanny, A.H. and Dougherty, B.P. (2001), "Building Integrated Photovoltaic Test Facility", *J. Sol. Energy-T.*, ASME, **123**(3), 194-199.
- Hall, B.H. and Khan, B. (2003), *Adoption of New Technology*, National Bureau of Economic Research, Cambridge, MA, USA.
- International Code Council (ICC) (2012), *International Energy Conservation Code, R-33*. ICC.
- Jakubiec, J.A. and Reinhart, C.F. (2013), "A method for predicting city-wide electricity gains from photovoltaic panels based on LiDAR and GIS data combined with hourly Daysim simulations", *Sol. Energy*, **93**, 127-143.
- Kawajiri, K., Oozeki, T. and Genchi, Y. (2011), "Effect of temperature on PV potential in the world", *Environ. Sci. Technol.*, **45**(20), 9030-9035.
- King, D.L. and Eckert, P.E. (1996), "Characterizing (rating) the performance of large photovoltaic arrays for all operating conditions", *Proceedings of '96 Photovoltaic Specialists Conference*, IEEE, Washington, DC, USA.
- King, D.L., Boyson, W.E. and Kratochvil, J.A. (2002), "Analysis of factors influencing the annual energy production of photovoltaic system", *Proceedings of '02 Photovoltaic Specialists Conference*, IEEE, New Orleans, LA, USA.
- Li, D.H., Yang, L. and Lam, J.C. (2013), "Zero energy buildings and sustainable development implications-a review", *Energy*, **54**, 1-10.
- Lubitz, W.D. (2011), "Effect of manual tilt adjustments on incident irradiance on fixed and tracking solar panels", *Appl. Eng.*, **88**(5), 1710-1719.
- Marion, B., Adelstein, J., Boyle, K., Hayden, H., Hammond, B., Fletcher, T., Canada, B., Narang, D., Kimber, A. and Mitchell, L. (2005), "Performance parameters for grid-connected PV systems", *Photovoltaic Specialists Conference, 2005, Conference Record of the Thirty-first IEEE*, Lake Buena Vista, FL, USA, January.
- Marion, W., Wilcox, S. and Andreas, A. (1994), *Solar Radiation Data Manual for Flat-Plate and Concentrating Collectors*, National Renewable Energy Laboratory, Golden, CO, USA.
- Marszal, A.J., Heiselberg, P., Bourrelle, J.S., Musall, E., Voss, K., Sartori, I. and Napolitano, A. (2011), "Zero energy building-a review of definitions and calculation methodologies", *Energy Build.*, **43**(4), 971-979.
- National Climatic Data Center (1998), *Climatic Wind data for the United States*, National Oceanic and Atmospheric Administration, ASHEVILLE, NC, USA.
- National Renewable Energy Laboratory (2008), *A Performance Calculator for Grid-Connected PV Systems*, National Renewable Energy Laboratory, <http://rredc.nrel.gov/solar/calculators/pvwatts/version1>.
- National Weather Service Forecast Office (2008), *Observed Weather, Des Moines, IA*, National Weather Service Forecast Office, <http://www.weather.gov/climate/index.php?wfo=dmx>.
- Norton, P., Christensen, C., Hancock, E., Barker, G. and Reeves, P. (2008), *The NREL/Habitat for Humanity Zero Energy Home: A Cold Climate Case Study for Affordable Zero Energy Homes Case Study Report*, National Renewable Energy Laboratory, Golden, CO, USA.
- Office of Energy Efficiency & Renewable Energy (EERE) (2014), *Report PNNL-SA-105477: New town builders: The AitiZEN Plan, Denver, CO*, Pacific Northwest National Laboratory, Richland, WA, USA.

- Revelle, W. (2006), *Lakeside Solar House*, <http://personality-project.org/r/r.plottingdates.html>.
- Sherwood, L (2014), *U.S. Solar Market Trends 2013*, Interstate Renewable Energy Council, Latham, NY, USA.
- Whitaker, C.M., Townsend, T.U., Wenger, H.J., Iliceto, A., Chimento, G. and Paletta, F. (1992), “Effects of irradiance and other factors on PV temperature coefficients”, *Proceedings of '91 Photovoltaic Specialists Conference, IEEE*, Las Vegas, NV, USA, October.
- Wilcox, S. and Marion, W. (2008), *Users Manual for TMY3 Data Sets*, National Renewable Energy Laboratory, Golden, CO, USA.

CC